Available online at www.sciencedirect.com
SCIENCE DIRECT®
Catalysis Today 86 (2003) 151–171
CATALYSIS TODAY
www.elsevier.com/locate/cattod

MgO-supported Mo, CoMo and NiMo sulfide hydrotreating catalysts

Miroslav Zdražil*

Institute of Chemical Process Fundamentals, Academy of Sciences of the Czech Republic, Rozvojová 135, CZ-165 02 Prague 6, Suchdol, Czech Republic

Received 5 February 2003; received in revised form 20 May 2003; accepted 23 May 2003

Abstract

The most common preparation of high surface area MgO (100–500 $m^2\ g^{-1}$) is calcination of $Mg(OH)_2$ obtained either by precipitation or MgO hydration or sol–gel method. Preparation of MoO_3/MgO catalyst is complicated by the high reactivity of MgO to H_2O and MoO_3. During conventional aqueous impregnation, MgO is transformed to $Mg(OH)_2$, and well soluble $MgMoO_4$ is easily formed. Alternative methods, that do not impair the starting MgO so strongly, are non-aqueous slurry impregnation and thermal spreading of MoO_3. Mo species of MoO_3/MgO catalyst are dissolved as $MgMoO_4$ during deposition of Co(Ni) by conventional aqueous impregnation. This can be avoided by using non-aqueous impregnation. Co(Ni)Mo/MgO catalysts must be calcined only at low temperature because Co(Ni)O and MgO easily form a solid solution. Literature data on hydrodesulfurization (HDS) activity of MgO-supported catalysts are often contradictory and do not reproduced well. However, some results suggest that very highly active HDS sites can be obtained using this support. Co(Ni)Mo/MgO catalysts prepared by non-aqueous impregnation and calcined at low temperature exhibited strong synergism in HDS activity. Co(Ni)Mo/MgO catalysts are much less deactivated by coking than their Al_2O_3-supported counterparts. Hydrodenitrogenation (HDN) activity of Mo/MgO catalyst is similar to the activity of Mo/Al_2O_3. However, the promotion effect of Co(Ni) in HDN on Co(Ni)Mo/MgO is lower than that on Co(Ni)Mo/Al_2O_3.

Keywords: Impregnation; MgO; Hydrodesulfurization

1. Introduction

The legislation limits of sulfur content in transportation of fuels and heating oils have been steadily decreasing recently. The limits for transportation of fuels will probably fall to several wppm level in about 5–10 years. Some proposals suggest that the sulfur limit in diesel fuel should be well below 50 wppm, even as low as 10 wppm [1]. In this connection, the terms "deep hydrodesulfurization" and "ultra-low sulfur fuels" have appeared in the literature recently. It is expected that the deep hydrodesulfurization (HDS) will be achieved at acceptable costs by a combination of several technological measures; improved catalysts should significantly contribute to this achievement [2].

One of the key parameters determining the activity of Mo, CoMo and NiMo HDS catalysts is the type of support. The conventional support is Al_2O_3, but other alternative supports such as SiO_2, active carbon, TiO_2, ZrO_2, zeolites and various mixed oxides have been studied as well (for reviews see [3–7]). MgO-supported catalysts have attracted much less attention.

* Tel.: +420-2-203-90288; fax: +420-2-209-20661.
E-mail address: zdrazil@icpf.cas.cz (M. Zdražil).

0920-5861/$ – see front matter © 2003 Elsevier B.V. All rights reserved.
doi:10.1016/S0920-5861(03)00409-7

2. Scope of the review

2.1. High surface area MgO

MgO is a very reactive and versatile material and the results on it and on Mo and Co(Ni)Mo catalysts supported on it are often contradictory and not well reproducible. For instance, some authors noted that their MgO and MoO_3/MgO samples showed "erratic" behavior in surface area measurements [8,9]. For that reason, a large part of this review will be devoted to preparation and properties of MgO support alone. MgO of high dispersity has also been studied in a large number of research projects not directly concerned with catalysis (for instance, the reactive MgO for removal of SO_2 from waste gases [10] and destructive adsorption of pollutants [11]). These papers were published in chemical engineering, inorganic chemistry and materials chemistry journals and it seems that they were not fully explored in the literature on hydrotreating. I will call attention to some of these papers in the present review.

The mixed oxide supports containing MgO (for instance, MgO–Al_2O_3 [8,12]) and the catalysts supported on them will not be discussed.

2.2. Catalysts

In the present review, the specific features of MgO and MgO-supported sulfides will be compared with the conventional support Al_2O_3 and Al_2O_3-supported sulfides.

Journal literature on MgO-supported sulfide catalysts is limited and we attempted to cover it in the present review completely (Mo/MgO [8,13–19], NiMo/MgO [8,20–22], CoMo/MgO [22]). Some of these papers do not primarily deal with MgO support and contain only a few pieces of relevant information (for instance, paper [15] deals mainly with the effect of the purity of the Al_2O_3 support).

Several patents have described CoMo/MgO HDS catalysts (for instance, [23]), often in connection with selective HDS of cracked naphtha with reduced saturation of olefins (for instance, [24–26]). Only selected patents that give details on catalyst preparation and testing are mentioned below.

The systems MoO_3/MgO, NiO/MgO and CoO/MgO (in oxide or reduced forms) have also been studied in connection with reactions other than HDS, such as steam reforming, CO_2 reforming, oxidation, oxidative dehydrogenation and oxidative coupling. However, the reaction temperature of these reactions is usually far above the temperature range 300–400 °C used in hydrotreating and the catalysts possess relatively low surface areas up to, say, 50 $m^2\,g^{-1}$. These papers will be mentioned only when they contain some information relevant to the temperature range up to about 450 °C.

The system MoO_3/MgO has also been studied as one case of "monolayer catalysts" (MoO_3, WO_3 or V_2O_5 supported over Al_2O_3, SiO_2, TiO_2, ZrO_2 or MgO), without connection to any particular reaction (for instance, [9,27,28]). Relevant information from such papers is included in the present review.

3. MgO support

3.1. Introduction

Al_2O_3 is an advanced support and its various versions optimized for specific processes are produced on an industrial scale. Papers on Al_2O_3-supported sulfides typically used Al_2O_3 provided by some producer of hydrotreating catalysts. Such Al_2O_3 support is available in the shaped form that provides very good mechanical strength and is chemically and texturally stable upon storage.

MgO support in the form (texture, shape, mechanical strength) optimized specially for catalytic application is generally not available. Table 1 shows that MgO of diverse, and sometimes not sufficiently specified, origin was used in papers on hydrotreating. Information about the mechanical strength was seldom given. As to papers on other reactions, some special materials were used beside laboratory-made MgO support: Japan Reference Catalyst JRC-MgO-1 (59 $m^2\,g^{-1}$, methanol oxidation) [29], commercial MgO support pellets from Engelhard (S_{BET} was not given, N_2O decomposition on CoO/MgO and CuO/MgO) [30], Magox Super Premium Grade MgO, Premier Refractories and Chemicals (100–130 $m^2\,g^{-1}$, oxidation of butane over MoO_3/MgO) [31]. High surface area MgO is chemically and texturally not stable upon storage in air (see below).

Table 1
Origin of MgO support used in papers on hydrotreating

Subject of paper	Origin of MgO support	S_{BET} ($m^2\,g^{-1}$)	Reference
HDS on MoS_2/MgO	Not reported	Not reported	[14]
Mo and NiMo catalysts supported on Al–Mg mixed oxides	Hydrolysis of $Mg(OEt)_2$/calcination at 500 °C	130	[8]
Support effects in HDS on MoS_2	Ube Industries	145	[15]
Decomposition of $(NH_4)_6Mo_7O_{24}$ supported on various supports	Laboratory-made (by not specified "aqueous way")	154	[19]
HDS over MoS_2/MgO	Hydration of MgO/calcination at 390 °C	210–270	[17]
Support effect in HDS over MoS_2	Nakarai Chemicals	51	[13]
HDS on Mo/MgO and NiMo/MgO	Hydration of MgO/calcination at 390 °C	250	[22]

The surface area, S_{BET}, of the Al_2O_3 supports used for hydrotreating catalysts is in the range 150–300 $m^2\,g^{-1}$. Of course, the mere value of S_{BET} is not sufficient for texture characterization and the volume of pores and their distribution are also important.

The MgO of surface area 100–500 $m^2\,g^{-1}$ is referred to as "high surface area MgO" in the present review. The value of S_{BET} was often the only parameter characterizing the texture of MgO support in catalytic literature. That is why the texture of supports and catalysts is mostly discussed only in terms of S_{BET} in the present work.

3.2. Preparation by calcination of $Mg(OH)_2$

Density of crystalline $Mg(OH)_2$ (brucite) and MgO (periclase) is 2.36 and 3.58 $g\,cm^{-3}$, respectively. About 50% contraction of the lattice occurs in dehydration; this leads to the development of cracks and crystal disintegration [32]. This results in surface area increase during $Mg(OH)_2$ calcination.

The equilibrium H_2O partial pressure above $Mg(OH)_2$ is 4.5, 22, 83, 259 and 688 kPa at the temperatures of 250, 300, 350, 400 and 450 °C, respectively (calculated using an equation from [10]). The minimum temperature needed for complete conversion to MgO depends on the dispersion of the starting $Mg(OH)_2$ and the efficiency of H_2O removal. Temperatures of 350–450 °C are sufficient to achieve the decomposition in a reasonable time of 1–10 h (for TGA curves see for instance, [10,33,34]; for kinetics of the decomposition at constant temperatures see, for instance, [10]).

The surface area of MgO prepared by calcination of $Mg(OH)_2$ is the result of the interplay of two opposite phenomena: it is increased by H_2O evolution and simultaneously reduced by sintering. Sintering begins already at the moment when the first MgO species are formed [10]. The sintering is promoted by increased temperature and by the presence of H_2O vapor [10,12,35]. The most important calcination variables are thus the rate of temperature increase, final temperature, time held at final temperature, and H_2O partial pressure, p_{H_2O}.

The critical value of p_{H_2O} at which the perceptible sintering occurs depends on temperature. The MgO of $S_{BET} = 220\,m^2\,g^{-1}$ was fairly stable for 2 h at high temperature of 1050 °C with the extremely low p_{H_2O} of 1 mPa, while it sintered to MgO of $S_{BET} = 40\,m^2\,g^{-1}$ with p_{H_2O} of 0.6 kPa. However, at 400 °C, it was fairly stable for 3 h even with p_{H_2O} of 0.6 kPa (the samples were treated in a batch reactor under vacuum chamber at fixed p_{H_2O}) [35]. The p_{H_2O} of 0.6 kPa corresponds to relative air humidity of 23% at 22 °C.

Some contact of the MgO emerging during calcination with the evolved H_2O cannot be avoided in principle, because H_2O is evolved inside the pores formed (cracks or interparticles spaces in crystal agglomerates). The above-mentioned equilibrium values of p_{H_2O} above $Mg(OH)_2$ show that high values of p_{H_2O} can be reached in pores when the evolved H_2O is not effectively removed. The choice of calcination reactor and its regime is of key importance.

The calcination of small samples in a batch reactor in vacuum provides very effective removal of the emerging H_2O. Water is removed by permeation (driving force for permeation is pressure gradient). Permeation is fast, precludes the development of any significant gradient of p_{H_2O} inside pores and keeps

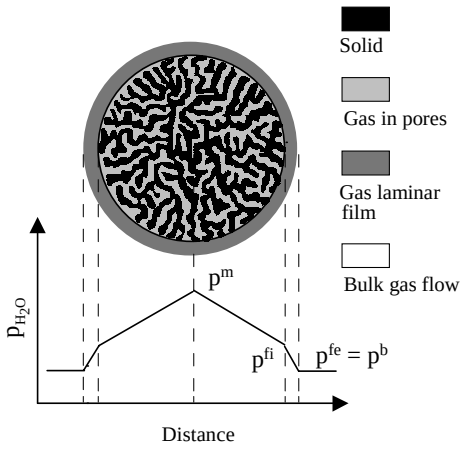

Fig. 1. Scheme of H_2O partial pressure, p_{H_2O}, during calcination of $Mg(OH)_2$ particle. p^m is the maximum p_{H_2O} in the particle center, p^{fi}, p^{fe} are the p_{H_2O} at internal and external surface of the gas laminar film surrounding the particle and p^b the p_{H_2O} in the bulk of gas.

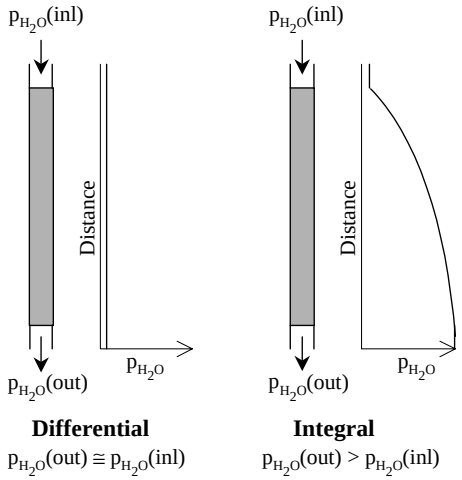

Fig. 2. Schemes of flow calcination reactor operated at differential and integral regime. p_{H_2O}(inl), p_{H_2O}(out) are the H_2O partial pressure at inlet and outlet of the reactor, respectively.

a low value of p_{H_2O} throughout the whole volume of calcined material. Sintering induced by H_2O is suppressed and high surface area MgO is obtained (see below). However, vacuum calcination of larger samples (above say 5 g) brings complications: a high capacity vacuum source is needed, heat transfer is slow and the solid layer might be non-isothermal during the temperature increase.

During calcinations at atmospheric pressure (in air or other gases), H_2O evolved in pores is transported to the bulk of gas surrounding the solid particle by diffusion, as shown in Fig. 1: by internal diffusion through the porous system from the solid particle interior to its external surface and by external diffusion across the laminar film of gas at the external surface of solid particle. The rate of transport depends on the effective diffusion coefficient, and the p_{H_2O} gradient across the solid particle, and the p_{H_2O} gradient across the laminar film. The effective diffusion coefficient has a finite value given by the dimensions of pores and the temperature and this value cannot be increased. However, the diffusion flow can be increased by a high p_{H_2O} gradient between solid particle interior and external surface of the laminar film. From this point of view, it is desirable to keep the p_{H_2O} at the external surface of the laminar film as low as possible.

The calcination in batch reactor in static air (or other gas) is an improper method. H_2O from interparticles spaces is transported into the air surrounding the layer of calcined material by bulk diffusion and convection (driving force for diffusion is p_{H_2O} gradient; driving force for convection is temperature gradient). This transport is relatively slow. The evolving H_2O pushes back the air from the layer of calcined material and the value of p_{H_2O} inside the layer can easily achieve atmospheric pressure (100 kPa).

Probably the most practical method is calcination in a reactor with a static bed of solid particles in flow of air (or an other gas) as shown in Fig. 2. In order to minimize the effect of the evolving H_2O, the reactor should be operated in the differential regime; this means with very high gas space velocity F/W, where F is the gas flow and W the sample mass. Proper pre-heating of the gas must be applied to operate the reactor in the isothermal regime at very high gas space velocity. In the differential regime, the axial gradient of p_{H_2O} across the solid particles bed is negligible (differential); the values of the reactor outlet and inlet p_{H_2O} are almost equal. The p_{H_2O} at the outer surface of gas laminar film is almost the same for all solid particles in the bed and it is almost equal to p_{H_2O} at the reactor inlet.

When the space velocity is insufficient, an axial gradient of p_{H_2O} is formed along the reactor (see Fig. 2) and sintering is promoted. Moreover, the downstream solid particles are in contact with the higher p_{H_2O} than

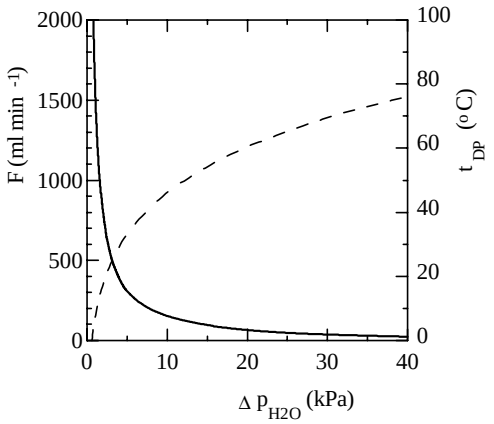

Fig. 3. Calcination in a flow reactor. Full line shows the gas flow F needed for the selected p_{H_2O} difference Δp_{H_2O} between the outlet and inlet; calcination of 10 g of $Mg(OH)_2$, temperature is increased in such a way that p_{H_2O} at the reactor outlet is constant and dehydration is complete after 4 h and dashed line the dew point t_{DP} at outlet when dry inlet gas is used.

the upstream particles and this may result in inhomogeneity of the MgO batch obtained.

Fig. 3 shows that a high flow of gas is needed to keep the reactor in the differential regime. Let us consider the calcination of 10 g of completely dry $Mg(OH)_2$ to MgO (3.1 g of H_2O must be removed) under a temperature program such that the outlet p_{H_2O}, p_{H_2O}(out), is kept constant and all H_2O is removed during 4 h. When the inlet air is completely dry, the flow to keep p_{H_2O}(out) at 1 kPa is 1591 ml min^{-1} (this p_{H_2O} corresponds to the usual 40% air relative humidity at 22 °C and no H_2O condensation occurs at the reactor outlet at 22 °C). When the ambient air of 50% relative humidity at 22 °C is sucked through the reactor, the reactor inlet H_2O partial pressure is 1.3 kPa. To achieve the p_{H_2O}(out) equal to the saturated p_{H_2O} at 22 °C of 2.6 kPa (no H_2O condensation occurs in the outlet tube at 22 °C), one needs a flow of air of 1237 ml min^{-1}; when the p_{H_2O}(out) is equal to saturated p_{H_2O} at 50 °C of 12.2 kPa (H_2O condensation occurs in the outlet tube at 22 °C), the flow of air needed is 132 ml min^{-1}.

It seems that the above facts were not fully considered in most papers concerned with MgO as catalytic support. A gap between chemical engineering and catalytic literature exists in this respect. For instance, the effects of gas (vacuum, air, H_2) and reactor shape (U-tube, vertical tube, sample holder of sorptometer) in $Mg(OH)_2$ calcination were studied and the differences in MgO surface area observed were ascribed to the "physical shape of the $Mg(OH)_2$ bed" [36]; however, neither gas flow nor the amount of the solid calcined were given. The space velocity used to prepare MgO by $Mg(OH)_2$ calcination was not given in the papers oriented to catalysis [8,9,16–21,36,37]. Some of these papers mentioned the flow of gas, but this is incomplete information for the description of the reactor regime—the information about the amount of $Mg(OH)_2$ calcined should also be given.

The rate of calcination temperature increase is also interconnected with the effect of H_2O. At too slow temperature increase, the ratio of the rates of H_2O evolution and of its removal by diffusion is low. The p_{H_2O} in pores is kept low, but the temperature ramp time is long and the material is in contact with H_2O for long time. At too fast temperature increase, the ratio of the rates of H_2O evolution and of its removal by diffusion is high. This can result in high p_{H_2O} in pores even when the calcination reactor operates in the differential mode.

Another important calcination variable is $Mg(OH)_2$ particle size. The use of fine particles prevents large p_{H_2O} gradients inside particles on the one hand, but leads to too high pressure drop in flow calcination reactor on the other hand. Calcination of too large particles of $Mg(OH)_2$ (say above 5 mm) might raise the inhomogeneous texture of the resulting MgO particles.

Al_2O_3 support is produced by calcination of Al hydroxide and H_2O vapor also negatively influences its texture. (For a recent discussion of this point from an industrial calcination point of view, see [38].) However, the effect of H_2O is not so dramatic as that for MgO.

3.2.1. *$Mg(OH)_2$ obtained by precipitation*

The starting $Mg(OH)_2$ was obtained by precipitation from solution of some Mg salt (nitrate [28,39], sulfate [36,40], or chloride [36,37,40]). Using the solution of $MgCl_2$, one must devote great care to $Mg(OH)_2$ precipitate washing, because residual Cl ions hinder the development of high S_{BET} of MgO during calcination [36,41,42].

Other research (for instance [10]) used commercial $Mg(OH)_2$ that is usually also prepared by precipitation, often from $MgCl_2$ solution.

Table 2
Preparation of high surface area MgO by calcination of precipitated $Mg(OH)_2$

Starting $Mg(OH)_2$			Calcination	Resulting MgO		Reference
Origin, starting salt	S_{BET} ($m^2\,g^{-1}$)	Crystal size (nm)		S_{BET} ($m^2\,g^{-1}$)	Crystal size (nm)	
Laboratory-made, $MgSO_4$	89	–	In vacuum, 350 °C, 5 h	310	–	[40]
			In vacuum, 500 °C, 5 h	280	–	
Laboratory-made, $MgCl_2$	1	–	In vacuum, 350 °C, 5 h	25	–	
Laboratory-made, $MgSO_4$	69	21	In vacuum, 500 °C	346	5	[36]
	65	11	Air, thin layer, 450 °C	305	–	
Laboratory-made, $MgCl_2$	35	20	In vacuum, 450 °C	320	–	
			In vacuum, 500 °C	227	6	
			Air, thin layer, 450 °C	100	–	
Commercial	14	–	N_2 flow, 350 °C	335	–	[10]
			N_2 flow, 400 °C	260	–	
Commercial	–	–	Air, 500 °C	241	–	[43]
Laboratory-made, $MgCl_2$	50	25	Air, 500 °C	105	8	[37]

Some examples of MgO obtained are presented in Table 2. As compared with $Mg(OH)_2$ prepared by sol–gel method having S_{BET} of 500–1000 $m^2\,g^{-1}$ (see below), the S_{BET} of the dried precipitated $Mg(OH)_2$ was relatively low, usually well below 100 $m^2\,g^{-1}$. However, as shown in Table 2, this does not obstruct the rise of high S_{BET} of MgO of 300–350 $m^2\,g^{-1}$, provided that the proper calcination method is used.

Calcination in vacuum usually led to a higher MgO surface area than calcination at atmospheric pressure. However, when the calcination reactor was operated in the differential regime, the surface area above 300 $m^2\,g^{-1}$ was achieved even by calcination at atmospheric pressure, similarly to the results obtained by calcination in vacuum (compare data of [10,36] in Table 2).

3.2.2. $Mg(OH)_2$ obtained by hydration of commercial MgO

Some examples of MgO obtained are presented in Table 3. The rate of MgO hydration to $Mg(OH)_2$ in liquid H_2O increases with increasing dispersion (S_{BET}) of the starting MgO [45,46]. S_{BET} of commercial MgO is relatively low, typically in the 10–50 $m^2\,g^{-1}$ range (see Table 3). Transformation to $Mg(OH)_2$ was performed by heating the slurry of MgO with H_2O to 80–100 °C, followed by drying at 100 °C [16–18,22,36,42]. The heating step before drying was sometimes omitted and the slurry was either filtered off before drying or the whole slurry was dried without filtration. However, a long heating of the slurry is probably not needed. A mere standing and drying of the MgO/H_2O paste at room temperature provided surface areas of 230–270 $m^2\,g^{-1}$ after calcination (see [17] in Table 3). The details of MgO/H_2O slurry preparation, filtration, drying and calcination are important with respect to the mechanical strength of the product (see below).

Surface area of the $Mg(OH)_2$ obtained by hydration of commercial MgO is not very different from the S_{BET} of the starting MgO and is only 10–50 $m^2\,g^{-1}$. However, MgO of S_{BET} around 300 $m^2\,g^{-1}$ can be obtained by calcination under proper calcination conditions (see Table 3).

3.2.3. $Mg(OH)_2$ obtained by sol–gel method

The material named as “nanocrystalline MgO” or “nano-MgO” was prepared by a method involving alkoxide-based sol–gel synthesis of $Mg(OH)_2$. Various versions of this method and MgO surface areas achieved are illustrated in Table 4.

Very high S_{BET} of $Mg(OH)_2$ of 800–1100 $m^2\,g^{-1}$ was obtained by sol–gel method using methanol/H_2O hydrolysis mixture and supercritical drying in autoclave ([11,48] in Table 4). However, when methanol/toluene/H_2O hydrolysis mixture was used, such high

Table 3
Preparation of high surface area MgO by calcination of $Mg(OH)_2$ obtained by hydration of commercial low surface area MgO

Starting MgO		$Mg(OH)_2$		Calcination	Resulting MgO	Reference
S_{BET} ($m^2\,g^{-1}$)	Method of hydration	S_{BET} ($m^2\,g^{-1}$)	Crystal size (nm)		S_{BET} ($m^2\,g^{-1}$)	
33	H_2O slurry at 100 °C, drying in air at 100 °C	57	14	In vacuum, 450 °C Air, 450 °C	336 211	[36]
16		23	21	In vacuum, 450 °C	300	
12 30	H_2O slurry at 80 °C, drying in air at 110 °C	33 –	–	Air, 400 °C	200 280	[42]
–	H_2O slurry at 80 °C, drying at 22 °C	–	–	Air flow, 400 °C	250–300	[16]
70	Kneaded and extruded paste MgO/H_2O, drying at 22 °C	–	–	Air flow, 390 °C	230–270	[17]
15–25	Impregnation by H_2O at 22 °C, drying in air at 110 °C	18	–	Air flow, 400 °C	317	[41]
63	Impregnation in H_2O	–	–	Air, 450 °C	218	[44]
68	Solution of NH_4OH at 22 °C, pH = 12, drying in vacuum at 50 °C	–	–	Air, 500 °C	150	[9]

S_{BET} of $Mg(OH)_2$ was obtained even by conventional drying in air and in vacuum (see [47] in Table 4).

The surface area of $Mg(OH)_2$ obtained by sol–gel method is by one order of magnitude higher than that of $Mg(OH)_2$ obtained by precipitation or by MgO hydration. It was claimed that calcination of such high surface area $Mg(OH)_2$ provides extremely dispersed material—"nanocrystalline MgO" with S_{BET} as high as $500\,m^2\,g^{-1}$ and the crystal size as low as 4 nm (Table 4). The highest S_{BET} and the smallest crystal size of MgO obtained from $Mg(OH)_2$ prepared by precipitation or by MgO hydration was around $350\,m^2\,g^{-1}$ and 5 nm, respectively (Tables 2 and 3). The very high dispersion of "nanocrystalline MgO" leads to its high reactivity, for instance, in adsorption of acid gases such as SO_2 or in destructive adsorption of organic molecules such as organophosphonates and chlorinated hydrocarbons [11,51–53]. However, the papers on the application of "nanocrystalline MgO" as the support for metallic and oxide catalysts are rare (for instance, V_2O_5/MgO for oxidative dehydrogenation of propane [48], NiO/MgO for CO_2 reforming of methane [37]). The use of "nanocrystalline MgO" prepared by sol–gel method to catalysis over sulfides has not yet been reported.

3.3. Other methods

MgO of surface area of $426\,m^2\,g^{-1}$ was obtained by calcination of $MgCO_3$ in vacuum at 350 °C [40]. An extremely high S_{BET} value of $550\,m^2\,g^{-1}$ resulted from the calcination of native magnesite ($MgCO_3$) in vacuum at 650 °C [40]. MgO of $S_{BET} = 170\,m^2\,g^{-1}$ was prepared by the decomposition of Mg hydroxycarbonate in air at 500 °C [12]. However, MgO obtained from Mg (hydroxy)carbonate has not been used in catalysis over sulfides.

A new method for the synthesis of high surface area metal oxides called "matrix-assisted preparation in activated carbons" has also been applied to MgO [54]. Active carbon was impregnated by an aqueous solution of $Mg(NO_3)_2$ and the carbon was removed (gasified) by calcination in air at 500 °C. The resulting MgO exhibited broad MgO patterns in XRD and its S_{BET} was $201\,m^2\,g^{-1}$.

3.4. Texture

The standard step before S_{BET} measurement by N_2 physisorption is "outgassing" in vacuum or in flow of air, usually at a temperatures between 150 and 350 °C.

Table 4
Preparation of high surface area MgO (often assigned as nanocrystalline MgO) by calcination of $Mg(OH)_2$ obtained by sol–gel method

$Mg(OH)_2$			Calcination	Resulting MgO		Reference
Sequence of preparation steps	S_{BET} ($m^2\,g^{-1}$)	Crystal size (nm)		S_{BET} ($m^2\,g^{-1}$)	Crystal size (nm)	
$Mg(OCH_3)_2$ hydrolysis in (a) methanol/water and (b) methanol/toluene/water; drying in static air, 22 °C; drying in vacuum, 22 °C; drying in air, 60 °C	(a) 581 and (b) 715–1011	–	–	–	–	[47]
$Mg(OCH_3)_2$ hydrolysis in methanol/toluene/water; supercritical drying in autoclave; drying in air, 110 °C	1100	–	He flow, 500 °C	380	4	[48]
$Mg(OCH_3)_2$ hydrolysis in methanol/water; supercritical drying in autoclave	–	–	In vacuum, 500 °C	355	–	[49]
$Mg(OH)_2$ hydrogel precipitation in water; hydrogel changed to alcogel by washing with ethanol; (a) supercritical drying in autoclave and (b) drying in N_2 flow, 270 °C	(a) – and (b) 52	(a) – and (b) 10	(a) Air, 500 °C and (b) N_2 flow, 500 °C	(a) 165 and (b) 197	(a) 11 and (b) 12	[37]
$Mg(OCH_3)_2$ hydrolysis in methanol/toluene/water; supercritical drying in autoclave	800–1000		In vacuum, 500 °C	250–500	4	[11]
$Mg(OCH_3)_2$ hydrolysis in methanol/ benzene/water; supercritical drying in autoclave	–		Not reported	285–407	–	[50]

Typical Al_2O_3 supports of $S_{BET} = 150$–$300\,m^2\,g^{-1}$ adsorb about 5–10 wt.% of H_2O from air during storage. That H_2O is removed by "outgassing" without any significant effect on support texture. The cycle "storage/outgassing" can be repeated, and the same value of S_{BET} is obtained.

The interaction of MgO support with ambient atmosphere during storage is deeper. It is not only mere surface adsorption of H_2O and CO_2, but also the reaction with the subsurface MgO layers. The mass increase during storage may reach rather high values of 30–40 wt.%, depending on MgO surface area [55]. Any "storage/outgassing" cycle represents to some extent an additional "hydration/calcination" cycle and may significantly change the texture. For that reason the literature data on MgO texture obtained by N_2 physisorption must be considered cautiously. All details about the storage and manipulation of the sample before the measurement should always be given.

The N_2 adsorption isotherms on typical Al_2O_3 supports belong to Type IV (according to IUPAC classification [56]), which is characteristic for mesoporous solids. Some examples are given in Fig. 4. The hysteresis is distinct and the hysteresis loop exhibits a relatively well-developed plateau above p/p_0 of about 0.8.

The papers reporting N_2 adsorption isotherms for high surface area MgO are not numerous; the typical examples are presented in Fig. 4. The relation between preparation conditions and texture parameters (surface area, pore volume, distribution of pores) is not fully understood.

The MgO samples obtained by calcination of $Mg(OH)_2$ prepared either by precipitation or by MgO hydration exhibited mainly features of Type II adsorption isotherm. This isotherm is characteristic for solids composed of finely divided non-porous particles [56]. Such MgO samples exhibited either no hysteresis loop [9] or only a very narrow hysteresis

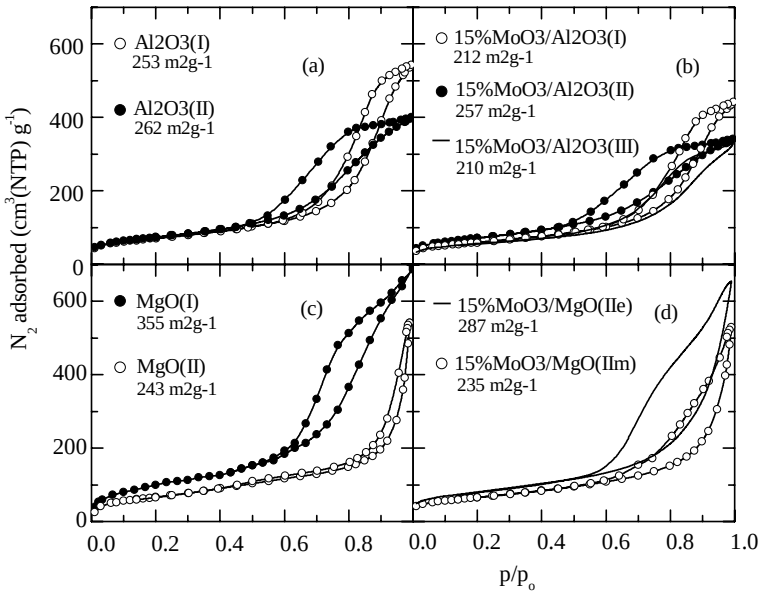

Fig. 4. Comparison of N_2 adsorption isotherms of MgO- and Al_2O_3-based systems. (a) Al_2O_3(I): AKZO HDS-000-1.5; Al_2O_3(II): Süd Chemie CS 331-1. (b) MoO_3/Al_2O_3(I) and MoO_3/Al_2O_3(II): laboratory-made [55]; MoO_3/Al_2O_3(III): BASF M8-30 [18]. (c) MgO(I): calcination of $Mg(OH)_2$ obtained by sol–gel method [49]; MgO(II): calcination of $Mg(OH)_2$ obtained by MgO hydration. (d) MoO_3/MgO(IIm) and MoO_3/MgO(IIe): slurry impregnation in methanol and ethanol, respectively [18].

loop ([32,44] and the sample of [18], Fig. 4). The hysteresis loop was of the Type H3 (according to IUPAC classification [56]), and the isotherms curves approached the *y*-axis asymptotically at $p/p_0 \rightarrow 1$. The volume of micropores determined by *t*-plot was very small (0–0.02 $cm^3\,g^{-1}$).

However, the MgO samples obtained by calcination of $Mg(OH)_2$ prepared by sol–gel method exhibited combined features of Types II and IV isotherms. A well-developed hysteresis loop and a hint of plateau at high p/p_0 were observed; micropores were absent (sample of [49], Fig. 4).

3.5. Shaping

Available data suggest that high surface area MgO can relatively easily be shaped into particles of reasonable mechanical strength needed for application in fixed bed reactors, at least for laboratory scale testing.

Nanocrystalline MgO was pelleted without significant loss of S_{BET} and porosity [53,57]. The material obtained by sol–gel method was pelleted either before calcination (as $Mg(OH)_2$) or after calcination (as MgO) and no significant differences in S_{BET} (it was about 340 $m^2\,g^{-1}$) or pore volume (it was about 0.7 $cm^3\,g^{-1}$) were observed.

Only soft MgO particles are usually obtained by the calcination of $Mg(OH)_2$ filter cake dried in an oven. However, hard particles were obtained when the cake was densified before drying and dried slowly at room temperature [16,17]. Densification can be made by pressing the cake on a Büchner funnel during vacuum filtration or by kneading the cake (or a $Mg(OH)_2/H_2O$ paste) in an agate mortar. The kneaded paste can also be extruded and after slow drying at room temperature, the hardness of the calcined extrudates is fairly good [17].

4. Catalysts

4.1. Introduction

The following necessary (but not sufficient) conditions must be fulfilled to obtain a good hydrotreating Mo, CoMo or NiMo catalyst. The support should

possess a large S_{BET} (say 150–300 $m^2\,g^{-1}$) and its texture should not be impaired during deposition of active species. The active components must be deposited in finely dispersed form. The reaction of the active components with the support bulk and the formation of large surface particles of the active components must be avoided. These fundamental goals are relatively easily achieved with Al_2O_3 support, but it is not quite so simple to fulfil them with MgO support.

4.1.1. Al_2O_3-supported catalysts

A "good" alumina with proper texture and composition (content of impurities or additives such as Na or Si) is the basis for the preparation of good hydrotreating catalysts by conventional aqueous impregnation using $(NH_4)_6Mo_7O_{24}$ and $Co(Ni)(NO_3)_2$ salts. If one starts with a commercial Al_2O_3 optimized for hydrotreating, it is not so difficult to achieve a high promotion effect between Co(Ni) and Mo and high activity (providing that some bad mistake, such as calcination largely above 500 °C, has not been made). All components tend toward "spontaneous" formation of active surface structures. In the oxide precursor, Mo species tend more toward surface monolayer formation and less to sintering. The diffusion of Mo species to the support bulk does not practically occur and the formation of $Al_2(MoO_4)_3$ is only very limited at calcination temperatures up to 500 °C. The tendency of Co(Ni) species toward sintering and the diffusion to the support bulk are also not too strong. References to original papers can be found for instance, in reviews [5,58,59].

Slight chemical "corrosion" of Al_2O_3 occurs during conventional impregnation (some Al ions are dissolved [60]) but this "corrosion" does not change the support texture significantly. The examples presented in Table 5 show that the surface areas of the resulting catalysts are practically the same as those of the starting Al_2O_3 support.

4.1.2. MgO-supported catalysts

The specific properties of MgO make the preparation of MgO-supported hydrotreating catalysts much more complicated than in the case of Al_2O_3.

High surface area MgO reacts easily with H_2O to form $Mg(OH)_2$ during aqueous impregnation. The rate of hydration is promoted by high dispersion of MgO. The conversion of MgO of $S_{BET} = 155\,m^2\,g^{-1}$ to $Mg(OH)_2$ was 86% after 15 min in water at 16 °C [45]. Moreover, after impregnation the wet catalyst is dried above room temperature (commonly up to 100 °C). It should be expected that the conversion of MgO to $Mg(OH)_2$ is almost complete after such treatment. MgO is again formed during subsequent calcination of the impregnated catalyst, but the resulting texture might be completely different from that of the original support (as illustrated below). The newly formed

Table 5
Change of S_{BET} during catalyst preparation by conventional aqueous impregnation using $(NH_4)_6Mo_7O_{24}$ and $Co(Ni)(NO_3)_2$

Support	Mo catalyst			Co(Ni)Mo catalyst			Reference
S_{BET} ($m^2\,g^{-1}$)	MoO_3 (wt.%)	S_{BET}[a] ($m^2\,g_{sup}^{-1}$)	Change (%)	Co(Ni)O (wt.%)	S_{BET}[a] ($m^2\,g_{sup}^{-1}$)	Change[b] (%)	
Al_2O_3							
333	13	334	0	–	–	–	[61]
174	13	167	−4	–	–	–	[61]
181	13	203	+12	–	–	–	[61]
185	13	190	+3	–	–	–	[62]
224	13	216	−3	2	208	−4	[8]
240	12	223	−7				[15]
MgO							
130	8	378	+190	–	183	−52	[8]
145	12	263	+81	–	–	–	[15]
150	19	333	+122	–	–	–	[9]
59	34	252	+326	–	–	–	[29]

[a] Surface area per 1 g of the support in the catalyst.
[b] Change during deposition of Co(Ni) on Mo catalyst.

MgO surface need not be covered by deposited Mo and Co(Ni) species.

Beside the reaction with H_2O in impregnation solutions, MgO also possesses much higher reactivity to metal salts in aqueous impregnation solutions than alumina. During calcination, the deposited Mo, Co and Ni salts and oxides react with the support bulk more easily in the case of MgO than in the case of Al_2O_3. This is discussed in the following sections.

4.2. Mo/MgO

4.2.1. Preparation by aqueous impregnation

The conventional impregnation by solution of $(NH_4)_6Mo_7O_{24}$ commonly used for Al_2O_3-supported Mo sulfide catalysts was also used in a majority of papers on MgO-supported sulfide catalysts [8,13–15,19]. However, in the case of MgO support, this method brings along serious complications.

The easy reaction of MgO with H_2O to $Mg(OH)_2$ was discussed above. Moreover, the natural pH of the impregnation solution of $(NH_4)_6Mo_7O_{24}$ (about 5.2–5.5) is well below the isoelectric point of MgO (about 12) and the solubility of MgO is considerable under these conditions. In a study of hydrotreating catalysts supported over Al_2O_3–MgO supports (not including pure MgO), separate particles of MgO were observed at the surface of some supports [63]. These MgO particles were dissolved as $MgMoO_4$ during impregnation and the molybdate then precipitated at the surface during drying. The solubility of $MgMoO_4$ is 14 g per 100 ml of water at 22 °C.

MgO of 59 $m^2\,g^{-1}$ surface area was impregnated by equilibrium adsorption from a solution of $(NH_4)_6Mo_7O_{24}$ [29,64]. The solution was filtered off after adsorption for 100 h at 50 °C. The dried catalyst contained 34 wt.% MoO_3. This value is far above the saturated adsorption loadings achieved over Al_2O_3 (typically 10–18 wt.% MoO_3 for Al_2O_3 of surface area 150–250 $m^2\,g^{-1}$). The only Mo species observed by Raman IR spectroscopy was $MgMoO_4$. All this indicates that Mo ions react easily with subsurface layers of MgO.

In order to prevent MgO dissolution, one can adjust the pH of the impregnation solution of $(NH_4)_6Mo_7O_{24}$ to 12 by addition of NH_4OH [9]. However, precaution did not prevent the reaction with water.

Ammonia ions of $(NH_4)_6Mo_7O_{24}$ are retained at Al_2O_3 surface during impregnation and drying and are removed only during calcination. However, in the case of MgO, NH_3 is evolved already during drying: it can be detected in the air above the heated impregnation slurry by smell or by wet litmus paper. Decomposition in flow of Ar of unsupported and Al_2O_3-supported $(NH_4)_6Mo_7O_{24}$ started at about 250 and 270 °C, respectively; however, the decomposition of MgO-supported $(NH_4)_6Mo_7O_{24}$ started already at about 100 °C [19].

Table 5 shows that S_{BET} values of the MoO_3/MgO catalysts prepared by aqueous impregnation were systematically much higher than S_{BET} values of the starting MgO. It is well known that sintering during calcination of hydroxides to oxides can generally be inhibited by the addition of foreign ions. For instance, the dispersion of MgO can be stabilized by Al ions [12]. The difference in S_{BET} of the resulting MoO_3/MgO and the starting MgO in Table 5 can be explained by the hydration of MgO to $Mg(OH)_2$ during impregnation and by the stabilizing effect of Mo anions during re-formation of MgO during calcination.

I conclude that aqueous impregnation of MgO by solution of $(NH_4)_6Mo_7O_{24}$ cannot be considered as the mere impregnation of an essentially stable support, as in the case of Al_2O_3. All data mentioned above show that complex chemical and physical transformations of MgO occur.

4.2.2. Preparation by non-aqueous impregnation

The texture of high surface area MgO is stable in organic solvents: dimethylsulfoxide (DMSO) [21] and methanol (ethanol) [18,21]. However, the solubility of $(NH_4)_6Mo_7O_{24}$ in these solvents is very low and thus the conventional solution impregnation (for instance, by pore filling method) is not feasible.

DMSO is probably the most powerful solvent of inorganic salts among non-aqueous solvents [65]. However, it is a high boiling solvent (boiling point is 189 °C) and transition metal ions catalyze its decomposition at increased temperatures. The blank impregnation of MgO (170 $m^2\,g^{-1}$) by DMSO followed by drying in a rotary vacuum evaporator at 150–170 °C did not change its surface area [21]. In the preparation of 12 wt.% MoO_3/MgO catalyst, the slurry of MgO and $(NH_4)_6Mo_7O_{24}$ in DMSO was dried in a rotary vacuum evaporator at 150–170 °C

[21]. It was assumed that $(NH_4)_6Mo_7O_{24}$ was dissolved at the beginning of drying and deposited on the MgO surface during the process. The surface area of the dried 15 wt.% MoO_3/MgO catalyst (without any in situ pre-treatment) was 72 $m^2\,g^{-1}$. The reason for that S_{BET} decrease was not given.

The solubility of $(NH_4)_6Mo_7O_{24}$ in methanol is very low. However, some evolution of NH_3 from the slurry of MgO (about 250 $m^2\,g^{-1}$) and $(NH_4)_6Mo_7O_{24}$ in methanol at room temperature was observed: litmus paper wetted by H_2O became blue in the vapor phase above the slurry [16]. This indicates that the dissolved $(NH_4)_6Mo_7O_{24}$ species react readily with MgO surface even when their concentration in methanol is very low. Mo ions are retained at the MgO surface, NH_3 is evolved and the additional solid $(NH_4)_6Mo_7O_{24}$ is dissolved. The gradual dissolution/reaction of $(NH_4)_6Mo_7O_{24}$ stops when the MgO surface is saturated by Mo species. The surface area of the resulting Mo/MgO catalysts was similar to that of the starting MgO (200–250 $m^2\,g^{-1}$). Such deposition of Mo species resembles the equilibrium adsorption impregnation method. However, the slurry of $(NH_4)_6Mo_7O_{24}$ is used instead of its solution and the method was named "slurry impregnation" [16,17].

The course of the reaction can be followed by three methods: (i) The evolved NH_3 was stripped from the reaction mixture by flow of air, absorbed in a H_2SO_4 solution and determined by titration [16]; (ii) MgO particles (0.16–0.32 mm) or extrudates (2.6 mm) reacted with the slurry of very fine $(NH_4)_6Mo_7O_{24}$ particles; the degree of $(NH_4)_6Mo_7O_{24}$ conversion was roughly evaluated from the disappearance of fine particles in the slurry [17]; (iii) MgO extrudates reacted with the slurry of fine $(NH_4)_6Mo_7O_{24}$ particles; the extrudates were separated from the slurry, washed with methanol and the MoO_3 concentration across the extrudates profile was determined by electron probe microanalysis (for more detail see below) [17].

The reaction of MgO with the slurry of $(NH_4)_6Mo_7O_{24}$ in methanol or ethanol was slow at room temperature: about 10 days were needed to deposit 15 wt.% of MoO_3 on MgO of surface area 210 $m^2\,g^{-1}$. However, the reaction time was considerably reduced by heating the mixture under reflux condenser: the MgO particles (0.16–0.32 mm, 250 $m^2\,g^{-1}$) were impregnated by 12 wt.% MoO_3 in about 5 h [16] and the MgO extrudates (diameter 2.6 mm, about 250 $m^2\,g^{-1}$) by 27 wt.% MoO_3 in about 20 h [17].

The interaction of MgO surface with dissolved $(NH_4)_6Mo_7O_{24}$ species in $(NH_4)_6Mo_7O_{24}$/MgO slurry is an irreversible reaction (very strong adsorption). For that reason, eggshell profiles of MoO_3 concentration across MgO particles are formed as illustrated in Fig. 5. The homogeneous profile was obtained only when enough $(NH_4)_6Mo_7O_{24}$ was used to saturate the whole surface and when the impregnation time was sufficiently long.

The maximum MoO_3 saturated loading achieved in slurry $(NH_4)_6Mo_7O_{24}$/methanol at room temperature was about 18–20 wt.% MoO_3 for MgO of surface area of about 250 $m^2\,g^{-1}$ (Fig. 5). The surface area occupied by one Mo atom at saturation was thus about 0.28–0.24 nm^2 Mo per atom. That corresponded reasonably well to the value observed in MoO_3 monolayer over Al_2O_3 [17] (the values for Al_2O_3 determined by various methods are summarized in [66]).

However, the maximum MoO_3 saturated loading achieved in the slurry $(NH_4)_6Mo_7O_{24}$/methanol at methanol boiling point (65 °C) was 27–30 wt.% MoO_3 with the MgO surface area of about 250 $m^2\,g^{-1}$ (Fig. 5). It was suggested that such a high value of the saturated loading is already not compatible with the concept of monolayer and that subsurface layers of MgO took part in the slurry impregnation [17].

The solubility in water of $(NH_4)_6Mo_7O_{24}$ is much higher than that of MoO_3: 42 versus 0.02 g MoO_3 per 100 ml at 25 °C, respectively. The solubility in methanol of $(NH_4)_6Mo_7O_{24}$ is very low and it should be assumed that the solubility of MoO_3 is even lower. However, it was observed that even the extremely low MoO_3 solubility is sufficient for the deposition of MoO_3 in the slurry MgO/MoO_3/methanol at room temperature (the MgO surface area was about 250 $m^2\,g^{-1}$ and the particle size fraction was 0.16–0.32 mm) [18]. The impregnation in non-aqueous methanol was slow (10 days at room temperature was not sufficient for the 15 wt.% MoO_3/MgO catalyst). The addition of 4 wt.% of water to methanol solvent did not hurt the MgO surface area and accelerated the impregnation (15 wt.% MoO_3/MgO catalyst was prepared in 10 days at room temperature). The XRD lines of the starting MoO_3 disappeared during impregnation, proving that Mo species are deposited in highly dispersed (monolayer) form. The attempt

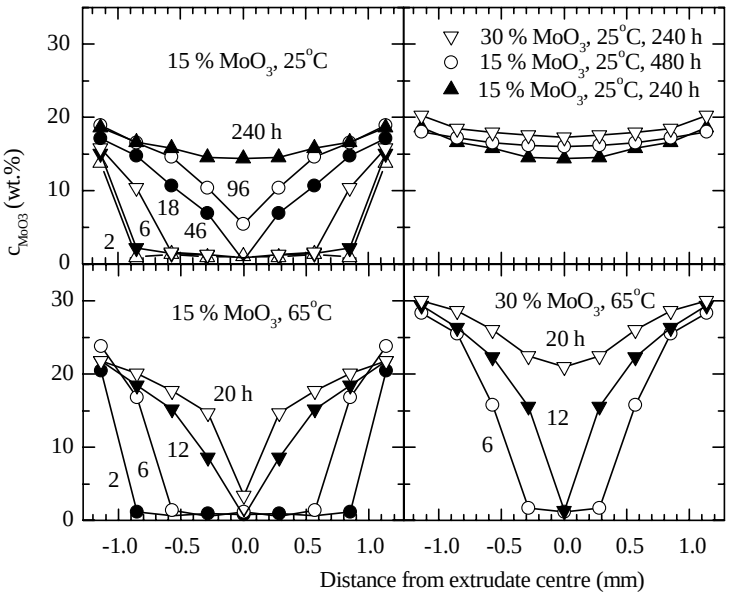

Fig. 5. Profiles of MoO_3 concentration c_{MoO_3} in MgO extrudates impregnated in the $(NH_4)_6Mo_7O_{24}$/methanol slurry at various nominal loadings, temperatures and times [17].

to increase the rate of impregnation by increasing the temperature to methanol boiling point was unsuccessful. The MgO particles (particles 0.16–0.32 mm or extrudates 2.6 mm) disintegrated during impregnation: surface layers of the particles peeled off, probably because of bulk $MgMoO_4$ formation.

The consecutive steps of slurry impregnation in the slurry MoO_3/MgO/(H_2O)methanol are dissolution of MoO_3, diffusion of dissolved Mo species into pores and reaction of dissolved MoO_3 species with MgO surface inside pores. It is not quite clear which of these steps is the rate-determining step. It can be expected that the use of very fine MoO_3 powder and small MgO particles should increase the rate of impregnation. The 15 wt.% MoO_3/MgO catalyst was prepared by the reaction of MoO_3 and MgO (250 $m^2\ g^{-1}$) in a kneaded paste with ethanol or aqueous methanol (4 wt.% H_2O). The reaction time used was 3 days at room temperature, but the minimum time needed to accomplish the reaction was not determined (it was probably shorter than 3 days) [18].

4.2.3. Preparation by other methods

One of the alternative methods of the deposition of MoO_3 over Al_2O_3 is "thermal spreading". The fine mechanical mixture of MoO_3 and Al_2O_3 is heated for several hours at a temperature of about 450–500 °C and the monolayer-type catalyst is obtained (for a recent survey of the literature, see [67]). This method has also been applied to MgO support [28]. The mixture of 5 wt.% MoO_3 with MgO of surface area 61 $m^2\ g^{-1}$ was heated at 450 °C for 24 h. It was found by laser Raman and Fourier transform infrared spectroscopies that the bulk MoO_3 reacted to the "surface molybdenum oxide species". The surface area of the resulting catalyst was not reported and the catalyst activity was not tested in any reaction.

4.2.4. Structure and texture

The nature of surface species in MoO_3/MgO catalyst has recently been discussed in review [27] and only short remarks will be given here. All the measurements reported in the literature have been made with the catalysts prepared by aqueous impregnation, except two studies [9,28] where some samples were prepared by heating the mixture of MgO and MoO_3 powders.

The predominating form of Mo species supported on Al_2O_3 is the surface monolayer of mono- and polymolybdate anions bound to the support via oxygen

bridges. $Al_2(MoO_4)_3$ is formed in appreciable amounts only after calcination at too high temperatures (above 500 °C); an appreciable amount of MoO_3 is formed only when the support is "overloaded". On the other hand, the preparation of the surface monolayer of molybdate anions over MgO is more difficult. It is not easy to avoid the formation of $MgMoO_4$ because it is produced not only during calcination, but also appears already during aqueous impregnation and drying. The reason for this difference is the much higher solubility of $MgMoO_4$ than of $Al_2(MoO_4)_3$. It should be assumed that any surface Mo–Mg–O species formed during impregnation is easily transformed to $MgMoO_4$ by dissolution/precipitation during standing and drying of the impregnation mixture. The crystalline MoO_3 (in the form detectable by XRD or LRS) was practically not observed in Mo/MgO catalysts prepared by aqueous impregnation, nor in "overloaded" samples. The reason is the high reactivity of MoO_3 to MgO both in the wet state during impregnation and in the dried state during calcination.

Strong interaction of Mo species with MgO support is documented by TPR results. Alumina supported Mo catalysts exhibit two main peaks. The positions of low- and high-temperature peaks reported in various papers were in the range 380–450 and 730–850 °C, respectively [8,61,68,69]. For MgO-supported catalysts they were shifted to 520–740 and 900–1200 °C regions, respectively [8,9,70]. Powdered $MgMoO_4$ was reduced at much higher temperature than MoO_3. The reduction of $MgMoO_4$ started only above 1100 °C while MoO_3 exhibited the reduction peak already at 750 °C [9].

For Al_2O_3-supported catalysts, the full sulfidation of Mo species is important for optimum activity. The formation of $Al_2(MoO_4)_3$ should be avoided because its sulfidation is difficult. No direct data are available on sulfidation of $MgMoO_4$. However, it was concluded that "the surface magnesium molybdate layers" are sulfided at the usual temperature of 400 °C and "continuous layers of MoS_2 around the magnesia particles" are formed [8]. The MoS_2 slabs in MgO-supported Mo catalyst seen by TEM were distinctly longer (about 8 nm) than in the catalysts supported on Al_2O_3 (2.5–4 nm) [8].

N_2 adsorption on MoO_3/MgO catalysts was measured for S_{BET} evaluation in several papers (see Tables 5 and 6) but few pictures of the adsorption isotherms were shown. The deposition of MoO_3 by

Table 6
Relative HDS activities of MgO- versus Al_2O_3-supported Mo sulfide catalysts

MoO_3/MgO		MoO_3/Al_2O_3		Reactant, temperature (°C), pressure (MPa)	Relative activity	Reference
MoO_3 (wt.%)	S_{BET} ($m^2\,g^{-1}$)	MoO_3 (wt.%)	S_{BET} ($m^2\,g^{-1}$)			
MoO_3/MgO prepared by aqueous impregnation						
8	329	13	199	Thiophene, 350, 0.1 Thiophene, 320, 0.1	0.71[a] 0.51[a]	[8]
12	231	12	196	Thiophene, 320, 1.8	0.47[b]	[15]
9	69	9	–	Thiophene, 350, 0.1	1.29[b]	[14]
10	154[c]	10	200[c]	Thiophene, 300, 0.1	0.51[b,d] 1.33[b,e]	[19]
10	51	10	170	Dibenzothiophene, 400, 6.9	0.26[a]	[13]
MoO_3/MgO prepared by non-aqueous impregnation						
15	235	15	210	Benzothiophene, 330, 1.6 Benzothiophene, 360, 1.6	1.02[f] 0.89[f]	[18]
11	250	15	210	Benzothiophene, 330, 1.6	0.95[a]	[16]

[a] Ratio of pseudo-first-order rate constants calculated from conversions given in the original paper.
[b] Ratio of rates given in the original paper.
[c] S_{BET} of the support, S_{BET} of the catalyst was not given.
[d] The catalysts were calcined at 550 °C in air.
[e] The catalysts were calcined at 550 °C in Ar.
[f] Ratio of rate constants given in the original paper.

thermal spreading and by aqueous impregnation did not change the character of isotherms; both the starting MgO and the MoO_3/MgO samples exhibited Type II isotherms showing no hysteresis, no micropores and no plateau at high p/p_0 (the isotherms were characterized by words, the pictures were not presented) [9]. However, as seen in Fig. 4, the deposition of MoO_3 by non-aqueous slurry impregnation changed the isotherms to some extent. The isotherm on the starting MgO(II) was essentially of Type II with very narrow hysteresis loop and no plateau at high p/p_0 (see Fig. 4c). On the other hand, the isotherms on the MoO_3/MgO(IIe) and MoO_3/MgO(IIm) samples exhibited relatively broad hysteresis loop that is characteristic for Type IV isotherm; however, plateau at high p/p_0 that is also characteristic for Type IV isotherm was absent (see Fig. 4d). None of the papers on MoO_3/MgO reported significant microporosity.

4.2.5. HDS activity

The literature data are summarized in Table 6. The activities of the Mo/MgO catalysts prepared by aqueous impregnation were mostly lower than the activities of Mo/Al_2O_3 [8,13,15,19]. However, taking into account the different content of MoO_3 in MgO- and Al_2O_3-supported catalysts, the activity at 350 °C of the MgO-supported catalyst prepared in [8] was not so bad. The good relative activity of Mo/MgO sample observed in [14] might be connected with the method of its presulfidation. The presulfidation by CS_2/H_2 mixture at 400 °C was used in that paper while the mixture H_2S/H_2 at 400 °C was used in the other papers shown in Table 6. Presulfidation by CS_2/H_2 mixture is probably accompanied by catalyst coking that is faster over Al_2O_3 than over MgO-supported catalysts. The reason for the exceptionally high activity of Mo/MgO catalyst calcined in argon ([19] in Table 6) is not clear. The authors suggested that calcination in argon reduced the mobility of Mo species as compared with calcination in air, which saved Mo species from the irreversible interaction with the support.

It is seen in Table 6 that the Mo/MgO catalysts prepared by non-aqueous impregnation exhibited similar activity to that of the Mo/Al_2O_3 system (a good commercial Mo/Al_2O_3 catalyst was used for comparison) [16,18].

The optimum catalytic activity of Mo/Al_2O_3 system is achieved only when the Mo species are fully sulfided. The interaction of MoO_3 with MgO is clearly stronger than that with Al_2O_3. The tendency to formation of $MgMoO_4$ is higher than in the case of $Al_2(MoO_4)_3$. It may be assumed that the full sulfidation of Mo/MgO is more difficult than that of Mo/Al_2O_3. However, this aspect has not been studied in the literature; the Mo/MgO catalysts in Table 6 were tested after sulfidation in H_2S/H_2 at 400 °C [8,13,16,18,19] and 450 °C [15], and in CS_2/H_2 at 400 °C [14].

4.3. CoMo/MgO and NiMo/MgO

4.3.1. Preparation by aqueous impregnation and HDS activity

The usual industrial method of Co(Ni)Mo/Al_2O_3 catalysts preparation is the impregnation of Al_2O_3 by the solution containing both Mo and Co(Ni) (pore filling co-impregnation). That method has not been tried for MgO support in journal literature but it has been used in some patents. The warm solution of $Co(NO_3)_2$ and $(NH_4)_6Mo_7O_{24}$ was added to MgO powder [25,26]. The resulting paste was dried, pilled to pellets and calcined at 430 °C. The use of about 1 wt.% of MoS_2 as a pilling agent and lubricant resulted in better mechanical strength of the pellets as compared with use of conventional agents such as graphite or stearates [24,26]. The resulting catalyst contained 3 wt.% CoO and 16 wt.% MoO_3 and its S_{BET} was only about 60 $m^2\,g^{-1}$ [26]. Nevertheless, its activity in HDS of cracked naphtha was higher and more stable as compared with the activities of conventional CoMo/Al_2O_3 catalysts containing 3 wt.% CoO and 15 wt.% MoO_3. The HDS conversions after 1 day on stream were 89 and 85%, respectively, and after 8 days on stream were 87 and 63%, respectively.

Another method, which is often used in laboratory research, is the impregnation of Mo/Al_2O_3 catalyst by a solution of Co(Ni) nitrate. The application of this method to MgO support brings specific complications. MoO_3/Al_2O_3 is practically insoluble in water or in impregnating Co(Ni) nitrate solution and behaves as an essentially stable support during impregnation. On the other hand, Mo/MgO is very unstable under aqueous impregnation conditions. MgO support is easily hydrated, as already discussed above. The aqueous slurry of equimolar amounts of MoO_3 and MgO fine powders reacts to give a clear solution

of $MgMoO_4$ in a few minutes at room temperature. It should be assumed consequently that any surface Mo–MgO species in Mo/MgO are easily dissolved as $MgMoO_4$ during the impregnation by Co(Ni) nitrate solution and subsequent drying.

Another complication is easy formation of CoO–MgO and NiO–MgO solid solutions. Firing at relatively low temperature of 500 °C was used to prepare the high surface area form of these materials (S_{BET} up to 100 $m^2\,g^{-1}$) [71,72]. It should be expected that with high surface area MgO, the formation of solid solution in several subsurface layers of MgO might occur even at temperatures below 500 °C.

The NiMo/MgO catalysts containing 8 wt.% MoO_3 and 1.8, 2.7 or 5.9 wt.% NiO were prepared by successive incipient wetness impregnations of MgO (130 $m^2\,g^{-1}$) by solutions of $(NH_4)_6Mo_7O_{24}$ and $Ni(NO_3)_2$ [8]. The catalysts were calcined at 500 °C for 4 h. It is seen in Table 5 that the S_{BET} value of the resulting NiMo/MgO catalyst was much smaller than that of the starting Mo/MgO. Such result once more illustrates the instability of MgO support during aqueous impregnation. The effect of Ni content on the catalyst activity is shown in Fig. 6. The first portion of added Ni was rather ineffective for promotion; this was explained by the formation of NiO–MgO solid solution during calcination. The relative activities and magnitudes of promotion are compared in Table 7 (conversions on NiMo catalysts were measured with the catalyst charge 0.05 g and were re-calculated to the charge 0.1 g using the first-order rate equation). Promotion in MgO-supported catalyst was improved by increasing NiO loading (Fig. 6), but still remained lower as compared with the Al_2O_3-supported system (Table 7). The relative activity of MgO- to Al_2O_3-supported NiMo catalysts was low (Table 7).

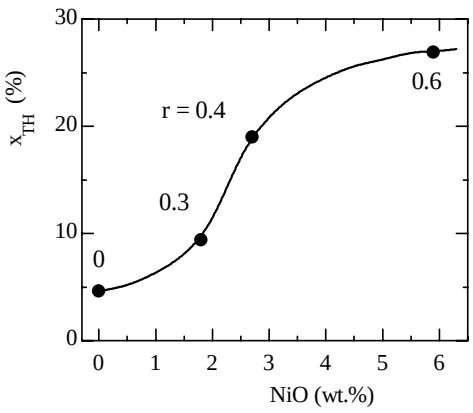

Fig. 6. Effect of NiO addition to the 8 wt.% MoO_3/MgO catalyst on thiophene HDS. x_{TH} is the conversion of thiophene at 350 °C, atmospheric pressure and 0.1 g of catalyst, r the atomic ratio Ni/(Ni + Mo). Calculated from data in [8].

Table 7
HDS of thiophene at 350 °C and atmospheric pressure [8][a]

Catalyst i[b]	x_{TH} (%)	$k_i/k_{NiMo/Al_2O_3}$	k_{NiMo}/k_{Mo}
13Mo/Al_2O_3	6.3	0.12	–
2.9Ni13Mo/Al_2O_3	43.0	1.00	8.6
8MoO_3/MgO	4.5	0.08	–
1.8Ni8Mo/MgO	9.4	0.18	2.1
5.9Ni8Mo/MgO	25.5	0.52	6.4

[a] Rate constants k were calculated from conversions x_{TH} using first-order kinetic equation.
[b] Composition is given in wt.% MoO_3 and NiO.

4.3.2. Preparation by non-aqueous impregnation and HDS activity

Co(Ni) nitrate is easily soluble in methanol and the impregnation of MoO_3/MgO by that solution is feasible without complications of aqueous impregnation. A high surface area 15 wt.% MoO_3/MgO (228 $m^2\,g^{-1}$, particle size 0.16–0.32 mm) was left standing with the solution of Co(Ni) nitrate in methanol [22]. The solution contained the amount of nitrate corresponding to 3.5 wt.% Co(Ni)O 15 wt.% MoO_3/MgO catalyst. The solution decolorized after 2 days of standing, indicating relatively strong adsorption of Co(Ni) cations. The S_{BET} of the resulting Co(Ni)Mo/MgO catalyst was measured after drying in a rotary vacuum evaporator at 100 °C (with no additional outgassing) and was about the same (±10%) as that of the starting Mo/MgO sample. The catalysts were calcined at low temperature of 350 °C (S_{BET} was not changed by calcination). The impregnation of the 15 wt.% MoO_3/MgO extrudates (diameter 2.8 mm) by the same procedure proved that the adsorption of Co(Ni) cations was not so strong as to cause the formation of eggshell profile of Co(Ni) concentration inside catalyst particles: a uniform distribution of Co(Ni) across the extrudates diameter was observed by electron probe microanalysis. The catalytic activity was tested in HDS of benzothiophene at 1.6 MPa; the results are summarized in Fig. 7 and Table 8.

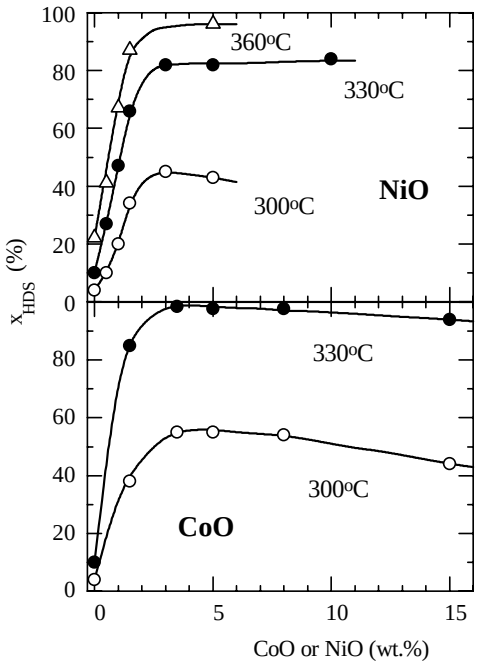

Fig. 7. Effect of CoO or NiO addition to the 15 wt.% MoO_3/MgO catalysts on benzothiophene HDS. x_{HDS} is the conversion of benzothiophene to ethylbenzene at 1.6 MPa, space time 6.5 g h mol^{-1}_{BT} [22].

In contradiction with the results shown in Fig. 6, the activity in Fig. 7 increased sharply already after the addition of small amounts of Co(Ni)O, and the strong promotion effect in the activity was achieved by the addition of 3–4 wt.% CoO or NiO. Different calcination temperatures, 500 and 350 °C, respectively, can explain this difference in data in Figs. 6 and 7. Very high sensitivity of the activity to the calcination temperature was observed: a sharp decrease of the activity (more than 50%) was observed when the calcination temperature was increased from 350 to 400 °C [22]. The optimum concentration of the promoters in Co(Ni)Mo/MgO catalysts seen in Fig. 7 falls into the range 3–4 wt.% CoO used in industrial Al_2O_3-supported catalysts.

The activities of the best CoMo/MgO and NiMo/MgO samples are compared with reference to industrial catalysts in Table 8. The activity of the Mo/MgO sample was about the same as that of the Mo/Al_2O_3 catalyst. However, because of the remarkably high synergistic effect between Co(Ni) and Mo in the MgO-supported Co(Ni)Mo catalysts, their activities were 1.5–2.3 times higher than the activities of their Al_2O_3-supported commercial counterparts (depending on catalyst and reaction temperature).

4.3.3. Other preparation methods and HDS activity

The catalyst containing 3 wt.% CoO, 12 wt.% MoO_3 and 85 wt.% MgO was prepared by mixing $Mg(OH)_2$, $Co(NO_3)_2$, $(NH_4)_6Mo_7O_{24}$ in aqueous paste [23]. The mixture was dried, pelleted and calcined at 550 °C for 2 h. The pore volume of the resulting catalyst was 0.38 $cm^3\,g^{-1}$ and its surface area was not reported. The activity was tested by HDS of hydrocarbon oils;

Table 8
HDS of benzothiophene at 1.6 MPa [22]

Catalyst	k_{HDS} (mmol $g^{-1}\,h^{-1}$)			Magnitude of synergism[a]		
	300 °C	330 °C	360 °C	300 °C	330 °C	360 °C
CoMo/MgO system						
3.5Co/MgO	1.3	3.1	6.4			
15Mo/MgO	4.8	13.7	32.7			
3.5Co15Mo/MgO	124	461	–	20	27	–
NiMo/MgO system						
3Ni/MgO	0.5	1.0	2.1			
15Mo/MgO	4.8	13.7	32.7			
3Ni15Mo/MgO	104	295	527	20	20	15
Reference Al_2O_3-supported catalysts						
15Mo/Al_2O_3 (BASF M8-30)	4.5	14.9	34.3			
3.5Ni19Mo/Al_2O_3 (Shell 324)	44.6	194	361	10	13	14
3.5Co15Mo/Al_2O_3 (Shell 344)	65.5	198	479	15	13	14

[a] For MgO-supported catalysts: $k_{Co(Ni)Mo}/(k_{Mo} + k_{Co(Ni)})$; for Al_2O_3-supported catalysts: $k_{Co(Ni)Mo}/k_{Mo}$.

Table 9
HDS of oils at 450 °C and 10 MPa [23]

Catalyst	HDS conversion (%)	
	Time on stream: 5 h	Time on stream: 300 h
Crude oil		
CoMo/MgO	97.1	87.5
CoMo/Al_2O_3	96.3	49.3
Lubrication oil		
CoMo/MgO	98.0	88.9
CoMo/Al_2O_3	98.0	65.8

the results are shown in Table 9. The initial activity (after 5 h on stream) of MgO and Al_2O_3 catalysts was about the same. However, the Al_2O_3-supported catalyst deactivated faster than the MgO-supported catalyst (presumably by coking). After 300 h on stream, the MgO-supported catalyst was much more active than the Al_2O_3-supported sample. When the rate constants are calculated from conversions in Table 9 using the first-order rate equation, the constants for HDS of crude and lubrication oil on the MgO-supported catalyst after 300 h on stream are 3 and two times higher than those for the Al_2O_3-supported sample, respectively.

4.3.4. Structure

The state of Co and Ni in oxide and sulfide Co(Ni)Mo/Al_2O_3 catalysts has been studied in detail (for review see [5,58,59,73]). However, practically no data are available on MgO-supported catalysts in this respect.

Typical MoS_2 slabs of one to three layers and lengths up to about 4 nm are observed by TEM/HREM in sulfided Ni(Co)Mo catalysts supported on Al_2O_3 [73,74]. Such slabs were found also on NiMo/MgO [8,75] and CoMo/MgO [75] catalysts, but they were distinctly longer, up to 8 nm. It is generally assumed that Ni decorates the edge planes of MoS_2 slabs and impedes their lateral growth. The presence of long slabs in NiMo/MgO catalysts was explained by low surface Ni concentration, which was indicated by small promotion effect and caused by formation of NiO–MgO solid solution [8]. However, the long slabs were also observed in Ni(Co)Mo/MgO catalysts that were calcined at low temperature and exhibited very high promotion [75].

Table 10
Relative activity in parallel HDS of thiophene, A_{HDS}, and HDN of pyridine, A_{HDN} [75]

Catalyst	A_{HDS}[a]	A_{HDN}[b]
MgO-supported catalysts		
3.5Co	–	–
3Ni	0.1	0.1
15Mo	1.2	1.0
3.5Co15Mo	10.5	1.4
3Ni15Mo	11.0	1.6
Al_2O_3-supported catalysts		
15Mo	1.0	1.0
3.5Co15Mo	4.6	1.8
3.5Ni19Mo	9.3	3.4

[a] Ratio of the first-order rate constants; the reference catalyst is the 15Mo/Al_2O_3 sample.

[b] Ratio of space times needed for HDN conversion of 20%; the reference catalyst is the 15Mo/Al_2O_3 sample.

4.4. Hydrodenitrogenation (HDN) activity

The MgO-supported catalysts of Table 8 prepared by non-aqueous impregnation were also tested in parallel HDN of pyridine and HDS of thiophene. The results are summarized in Table 10 and Fig. 8.

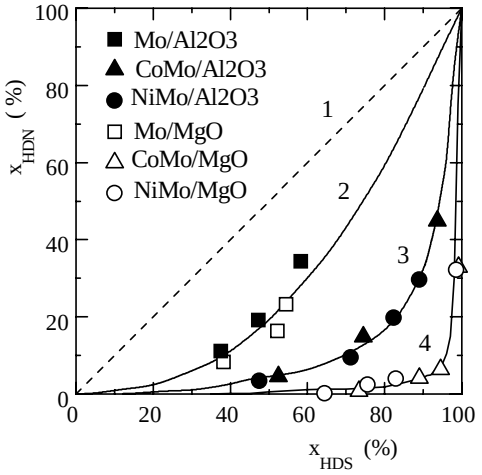

Fig. 8. Comparison of HDN/HDS selectivity of MgO- and Al_2O_3-supported catalysts in parallel HDN of pyridine and HDS of thiophene. x_{HDN} and x_{HDS} are conversions, 320 °C, 2 MPa, the feed contained 220 and 240 molar ppm of pyridine and thiophene, respectively. (1) A hypothetical catalyst of the same HDN and HDS activities; (2) Mo catalysts; (3) Co(Ni)Mo/Al_2O_3 catalysts; (4) Co(Ni)Mo/MgO catalysts [75].

The promotion effect in HDS on MgO-supported catalysts was strong and Co(Ni)Mo/MgO catalysts were more active than their Al_2O_3-supported counterparts (Table 10). HDN activity values of Mo/MgO and Mo/Al_2O_3 samples were about the same. However, the promotion in HDN activity on MgO-supported catalysts was weaker than in Al_2O_3-supported samples and Co(Ni)/MgO samples were less active than Co(Ni)Mo/Al_2O_3 catalysts.

Fig. 8 shows that HDN/HDS selectivity of Mo/MgO and Mo/Al_2O_3 catalysts was about the same. However, the opposite ranking of MgO- versus Al_2O_3-supported bimetallic catalysts in HDS and HDN activities led to pronounced differences in HDN/HDS selectivity of these two systems. The HDN/HDS selectivity of the Co(Ni)Mo/MgO systems was extremely low (Fig. 8).

It is generally believed that catalyst acidity promotes adsorption of basic nitrogen compounds and splitting of the C–N bond [5,59]. The poor performance in HDN of bimetallic Co(Ni)Mo/MgO catalysts can then be explained by basicity of the support. However, this conclusion is challenged by the behavior of the Mo/MgO catalyst, which was as active as the Mo/Al_2O_3 sample.

5. Conclusions

Relatively little attention has so far been devoted to MgO-supported sulfide hydrotreating catalysts. However, general considerations suggest that further research on them may be of interest. MgO is a common, easily attainable and not expensive material. Highly dispersed and porous MgO can be prepared by several alternative procedures, some of which are relatively simple. Such MgO materials (and also its $Mg(OH)_2$ precursor) are currently studied for application as adsorbent, reinforcing filler, flame-retardant filler, thermal insulator or precursor of advanced ceramic materials. The results of these studies can be utilized with advantage in catalytic research. Available data suggest that the shaping of MgO into particles suitable for catalytic reactors should be not difficult. It can be assumed that the basicity of MgO is an advantage as compared with neutral or acidic supports. Oxide and sulfide Mo species are acidic and thus the basic support should keep them in highly dispersed form. Surface basicity should keep down coking, which is intensive on Al_2O_3-supported catalysts and deactivates them. MgO basicity may promote formation of short edge-bonded MoS_2 slabs (each edge plane possesses Lewis acidity) and may thus increase the edge plane area suitable for promotion by Co(Ni).

However, the data published up to now are not sufficient for full confirmation of the above considerations, even though some results are fairly encouraging. It appears that the problem is to find out a proper preparation procedure. The material chemistry of MgO is so specific among other supports that the preparation of MgO-supported sulfides requires new and special approaches. The most important differences between MgO- and Al_2O_3-supported systems are the following. MgO exhibits typically Type II N_2 adsorption isotherm (characteristic for fine non-porous particles) while Al_2O_3 exhibits typically Type IV isotherm (characteristic for mesoporous materials). MgO is easily hydrated and hydration leads to its complete structural and textural reconstruction. Soluble $MgMoO_4$ is easily formed from MgO and MoO_3 in water even at room temperature. Co(Ni) ions diffuse extensively into MgO bulk at relatively low temperatures of about 400–500 °C. A routine application of preparation steps established in catalysis over sulfides supported on other supports may often damage MgO support and the active structures in MgO-supported catalysts. For instance, the calcination temperature of 400–500 °C that is safe for Co(Ni)Mo/Al_2O_3 catalyst seems to be far too high for Co(Ni)Mo/MgO catalyst.

It can be speculated that two main approaches, already applied in the literature, may be further developed in future research. The first one would start with the MgO support optimized not only as to S_{BET} but also as to pore size distribution. It seems that such support might be obtained by optimized calcination of a proper form of $Mg(OH)_2$. The next step would be to improve the methods of Mo and Co(Ni) deposition that do not impair the support (for instance, non-aqueous impregnation or thermal spreading). Another approach may be further exploration of such a method in which the step of support preparation is combined with active metals deposition (for instance, calcination of the paste of $Mg(OH)_2$ with Co(Ni) and Mo oxides or their precursors).

Acknowledgements

Support by the Grant Agency of the Czech Republic (Grant 104/01/0544) is gratefully acknowledged.

References

[1] R.R. Bharvani, R.S. Henderson, Hydrocarb. Process. 81 (2002) 61.
[2] W.K. Shifleft, L.D. Krenzke, Hydrocarb. Process. 81 (2002) 41.
[3] F. Luck, Bull. Soc. Chim. Belg. 100 (1991) 781.
[4] M. Breysse, J.L. Portefaix, M. Vrinat, Catal. Today 10 (1991) 489.
[5] H. Topsøe, B.S. Clausen, F.E. Massoth, Hydrotreating Catalysis, Science and Technology, Springer, Berlin, 1996.
[6] P.T. Vasudevan, J.L.G. Fierro, Catal. Rev.-Sci. Eng. 38 (1996) 161.
[7] L.R. Radovic, F. Rodríguez-Reinoso, Chem. Phys. Carbon 25 (1997) 243.
[8] T. Klimova, D.S. Casados, J. Ramírez, Catal. Today 43 (1998) 135.
[9] J.M.M. Llorente, V. Rives, P. Malet, F.J. Gil-Llambías, J. Catal. 135 (1992) 1.
[10] M. Hartman, O. Trnka, V. Veselý, AIChE J. 40 (1994) 536.
[11] K.J. Klabunde, J. Stark, O. Koper, C. Mohs, D.G. Park, S. Decker, Y. Jiang, I. Lagadic, D. Zhang, J. Phys. Chem. 100 (1996) 12142.
[12] H. Schaper, J.J. Berg-Slot, W.H.J. Stork, Appl. Catal. 54 (1989) 79.
[13] H. Shimada, T. Sato, Y. Yoshimura, J. Haraishi, A. Nishijima, J. Catal. 110 (1988) 275.
[14] K.V.R. Chary, H. Ramakrishna, K.S. Rama Rao, G. Murali Dhar, P. Kanta Rao, Catal. Lett. 10 (1991) 27.
[15] M.J. Ledoux, A. Peter, E.A. Blekkan, F. Luck, Appl. Catal. A 133 (1995) 321.
[16] T. Klicpera, M. Zdražil, Catal. Lett. 58 (1999) 47.
[17] T. Klicpera, M. Zdražil, J. Mater. Chem. 10 (2000) 1603.
[18] T. Klicpera, M. Zdražil, Appl. Catal. A 216 (2001) 41.
[19] C. Thomazeau, V. Martin, P. Afanasiev, Appl. Catal. A 199 (2000) 61.
[20] V. Koloušek, P. Pálka, E. Hillerová, M. Zdražil, Colect. Czech. Chem. Commun. 56 (1991) 580.
[21] E. Hillerová, Z. Vít, M. Zdražil, Appl. Catal. A 118 (1994) 111.
[22] T. Klicpera, M. Zdražil, J. Catal. 206 (2002) 314.
[23] S. Kurokawa, T. Miyasaki, Jpn. Patent 75,114,405 (1975); Chem. Abstr. 84 (1976) 47020f.
[24] A.P. Yu, E.C. Myers, US Patent 4,132,632 (1979); Chem. Abstr. 90 (1979) 124392g.
[25] R.J. Bertolacini, T.A. Sue-A-Quan, US Patent 4,140,626 (1979); Chem. Abstr. 90 (1979) 189614a.
[26] R.J. Bertolacini, US Patent 4,203,829 (1980).
[27] G. Mestl, T.K.K. Srinivasan, Catal. Rev.-Sci. Eng. 40 (1998) 451.
[28] S.R. Stampfl, Y. Chen, J.A. Dumesic, Ch. Niu, C.G. Hill, J. Catal. 105 (1987) 445.
[29] D.S. Kim, I.E. Wachs, K. Segawa, J. Catal. 146 (1994) 268.
[30] R.S. Drago, K. Jurczyk, N. Kob, Appl. Catal. B 13 (1997) 69.
[31] G.E. Vrieland, C.B. Murchison, Appl. Catal. A 134 (1996) 101.
[32] M.M.L. Ribeiro Carrott, P.J.M. Carrott, N.N. Brotas de Carvalho, K.S.W. Sing, Stud. Surf. Sci. Catal. 62 (1991) 635.
[33] J.A. Wang, O. Novaro, X. Bokhimi, T. López, G. Gomez, J. Navarrete, M.E. Llanos, E. Lopez-Salinas, Mater. Lett. 35 (1998) 317.
[34] E. Alvarado, L.M. Torres-Martinez, A.F. Fuentes, P. Quintana, Polyhedron 19 (2000) 2345.
[35] P.J. Anderson, P.L. Morgan, Trans. Faraday Soc. 60 (1964) 930.
[36] S.E. Wanke, R.M.J. Fiedorov, Stud. Surf. Sci. Catal. 39 (1987) 601.
[37] B.-Q. Xu, J.-M. Wei, H.-Q. Sun, Q.-M. Zhu, Catal. Today 68 (2001) 217.
[38] K. Johansen, Stud. Surf. Sci. Catal. 143 (2002) 1.
[39] T. Matsuda, J. Tanabe, N. Hayashi, Y. Sasaki, H. Miura, K. Sugiyama, Bull. Chem. Soc. Jpn. 55 (1982) 990.
[40] R.I. Razouk, R.S. Mikhail, J. Phys. Chem. 63 (1959) 1050.
[41] G. Leofanti, M. Solari, G.R. Tauszik, F. Garbassi, S. Galvagno, J. Schwank, Appl. Catal. 3 (1982) 131.
[42] T.E. Holt, A.D. Logan, S. Chakraborti, A.K. Datye, Appl. Catal. 34 (1987) 199.
[43] M.A. Aramendía, V. Borau, C. Jiménez, J.M. Marinas, R. Roldán, F.J. Romero, F.J. Urbano, Stud. Surf. Sci. Catal. 143 (2002) 899.
[44] C. Martín, P. Malet, V. Rives, G. Solana, J. Catal. 169 (1997) 516.
[45] M. Maryška, J. Bláha, Ceram-Silikaty 41 (1997) 121.
[46] V.S. Birchal, S.D.F. Rocha, M.B. Mansur, V.S.T. Ciminelli, Can. J. Chem. Eng. 79 (2001) 507.
[47] Y.L. Diao, W.P. Walawender, C.M. Sorensen, K.J. Klabunde, T. Ricke, Chem. Mater. 14 (2002) 362.
[48] C. Pak, A.T. Bell, T.D. Tilley, J. Catal. 206 (2002) 49.
[49] V.B. Fenelonov, M.S. Mel'gunov, I.V. Mishakov, R.M. Richards, V.V. Chesnokov, A.M. Volodin, K.J. Klabunde, J. Phys. Chem. B 105 (2001) 3937.
[50] S.J. Teichner, G.A. Nicolaon, M.A. Vicarini, G.E.E. Gardes, Adv. Colloid. Interf. 5 (1976) 245.
[51] A. Khaleel, P.N. Kapoor, K.J. Klabunde, Nanostruct. Mater. 11 (1999) 459.
[52] I.V. Mishakov, A.F. Bedilo, R.M. Richards, V.V. Chesnokov, A.M. Volodin, V.I. Zaikovskii, R.A. Buyanov, K.J. Klabunde, J. Catal. 206 (2002) 40.
[53] E. Lucas, S. Decker, A. Khaleel, A. Seitz, S. Fultz, A. Ponce, W.F. Li, C. Carnes, K.J. Klabunde, Chem. Eur. J. 7 (2001) 2505.
[54] M. Schwickardi, T. Johann, W. Schmidt, O. Busch, F. Schüth, Stud. Surf. Sci. Catal. 143 (2002) 93.
[55] D. Gulková, O. Šolcová, T. Klicpera, M. Zdražil, in: Proceedings of the Sixth Pannonian International Symposium on Catalysis, Obergurgl, Austria, September 11–14, 2002, p. 158 (Book of abstracts).

[56] S.J. Gregg, K.S.W. Sing, Adsorption, Surface Area and Porosity, Academic Press, London, 1982.
[57] R. Richards, W.E. Li, S. Decker, C. Davison, O. Koper, V. Zaikovski, A. Volodin, T. Ricker, K.J. Klabunde, J. Am. Chem. Soc. 122 (2000) 4921.
[58] J. Grimblot, Catal. Today 41 (1998) 111.
[59] R. Prins, Adv. Catal. 46 (2001) 399.
[60] X. Carrier, J.F. Lambert, M. Che, J. Am. Chem. Soc. 119 (1997) 10137.
[61] Y. Okamoto, et al., Appl. Catal. A 170 (1998) 315.
[62] M.C. Abello, M.F. Gomez, O. Ferretti, Appl. Catal. A 207 (2001) 421.
[63] S. Houssenbay, E. Payen, S. Kasztelan, J. Grimblot, Catal. Today 10 (1991) 541.
[64] D.S. Kim, K. Segawa, T. Soeya, I.E. Wachs, J. Catal. 136 (1992) 539.
[65] W.S. MacGregor, in: A. Standen (Ed.), Kirk-Othmer Encyclopedia of Chemical Technology, vol. 19, Interscience, New York, 1969, p. 320.
[66] E. Hillerová, H. Morishige, H. Inamura, M. Zdražil, Appl. Catal. A 156 (1997) 1.
[67] H. Knözinger, E. Taglauer, in: G. Ertl, H. Knözinger, J. Weitkamp (Eds.), Handbook of Heterogeneous Catalysis, vol. 1, Wiley, Weinheim, 1997, p. 216.
[68] Y. Okamoto, et al., Appl. Catal. A 170 (1998) 329.
[69] R. López Cordero, F.J. Gil Llambias, A. López Agudo, Appl. Catal. 74 (1991) 125.
[70] M.L. Pacheco, J. Soler, A. Dejoz, J.M. López Nieto, J. Herguido, M. Menéndez, J. Santamaría, Catal. Today 61 (2000) 101.
[71] A. Cimino, F.S. Stone, in: G. Ertl, H. Knözinger, J. Weitkamp (Eds.), Handbook of Heterogeneous Catalysis, vol. 2, Wiley, Weinheim, 1997, p. 845.
[72] V.F. Kiselev, O.V. Krylov, Adsorption and Catalysis on Transition Metals and Their Oxides, Springer, Berlin, 1989.
[73] S. Eijsbouts, Appl. Catal. A 158 (1997) 53.
[74] E.J.M. Hensen, P.J. Kooyman, Y. van der Meer, A.M. van der Kraan, V.H.J. de Beer, J.A.R. van Veen, R.A. van Santen, J. Catal. 199 (2001) 224.
[75] J. Cinibulk, P.J. Kooyman, Z. Vít, M. Zdražil, Catal. Lett. 89 (2003) 147.